Eur. Phys. J. B **43**, 439–444 (2005)
DOI: 10.1140/epjb/e2005-00076-8

THE EUROPEAN PHYSICAL JOURNAL B

First-principles study of the optical properties of pure α-Al_2O_3 and La aluminates

S.M. Hosseini[a], H.A. Rahnamaye Aliabad, and A. Kompany

Department of Physics, Ferdowsi University of Mashad (Electroceramic and Material Laboratory), Mashhad, Iran

Received 1st September 2004 / Received in final form 8 November 2004
Published online 30 March 2005 –

Abstract. The optical properties of high k-gate α-Al_2O_3 and the effect of doping La have been studied by first principles using the density functional theory. The calculations were performed using the full potential–linearized augmented plane wave (FP-LAPW) method with the generalized gradient approximation (GGA). The calculated optical properties and EEL spectrum yield a static refractive index of 1.64 and a plasmon energy of 21.6 eV for pure α-Al_2O_3. Substitution of La for Al increases the static refractive index to 1.73, but decreases the plasmon energy to 17.8 eV for the $Al_{1.5}La_{0.5}O_3$ molecule.

PACS. 31.15.Ar Ab initio calculations (atoms and molecules) – 78.20.-e Optical properties of bulk materials and thin films – 78.20.Ci Refractive index

1 Introduction

The optical properties of the thermodynamically stable α-Al_2O_3, alumina, are of major interest because of its variety of applications as a structural ceramic and optical material. Alumina can also be used in combination with silicon dioxide layers to form multilayer structures with high damage thresholds in UV laser applications. Also, single crystal sapphire has good thermal properties, together with excellent electrical and dielectric properties.

The modeling of electronic and optical properties, by means of first-principles calculations, has become a very useful tool for understanding the properties of materials such as Al_2O_3. There have been some efforts in determining the optical properties of Al_2O_3 from either ab-initio [1–3] and by experimental methods such as vacuum ultraviolet (VUV) spectroscopy and electron energy-loss spectroscopy (EELS) [4–7]. However, most of the studies up to now have been for pure Al_2O_3 and to our knowledge there is no theoretical or experimental data reported for the optical properties of La aluminates. In this work, the optical properties of pure alumina have been calculated and the results of the influence of doping La on the optical properties of alumina are presented.

2 Method of calculation

The corundum structure consists of hexagonal close packed O atoms with cations filling up to two-thirds of the central octahedral sites. The hexagonal Al_2O_3 structure can be built up by placing close-packed planes of oxygen and aluminum ions, but this would give equal numbers of atoms, so one third of the Al sites must be empty. The most convenient unit cell of α-alumina is a rhomboheral prism comprising of six such (0001) oxygen planes separated by the associated pair of aluminum planes. The cell contains just one Al atom and three O atoms in each plane.

Typically Al atoms are in the center of tetrahedrally and octahedrally coordinated sites with 4 and 6 atoms respectively, the most widely known crystal structure of α-Al_2O_3 contains all Al atoms in octahedral coordination and we chose to study this structure. The α-Al_2O_3 (corundum) structure, Figure 1, prepared by XCrySDen [8] belongs to the space group R-3c (number: 167)

The unit cell used for $Al_{1.5}La_{0.5}O_3$ is shown in Figure 2. It consists of six oxygen layers of O1, O2, O3, O4, O5, O6 with 18 oxygen atoms in total, plus nine Al layers Al1, Al2, Al3, Al4, Al5, Al6, Al7, Al8, Al9 with 9 Al atoms and three La layers La1, La2, La3 with three atoms all in octahedral positions, resulting in 30 atoms in the unit cell. We assume that the substitutions of La for Al (most likely), might occur at octahedral sites within the alumina structure. The lattice constant for this structure is $a = b = 8.98$ a.u, $c = 24.54$ a.u (1 a.u = 0.529 Å).

The calculations of the electronic and optical properties of α-Al_2O_3 and $Al_{2-x}La_xO_3$ were carried out with a self-consistent scheme by solving the Kohn-Sham equation using a FP-LAPW method in the framework of the DFT along with the generalized gradient approximation (GGA) [9,10] by WIEN2k package [11].

In the FP-LAPW method, space is divided into two regions, a spherical "muffin-tins" around the nuclei in which

[a] e-mail: sma_hosseini@yahoo.com

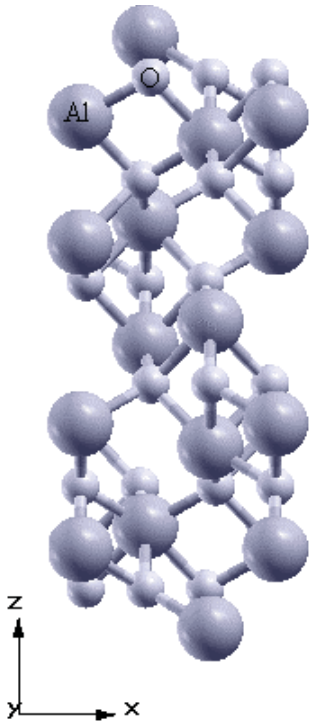

Fig. 1. Structure of α-Al_2O_3. The large circle represents the Al atoms. and the small one represents the O atoms.

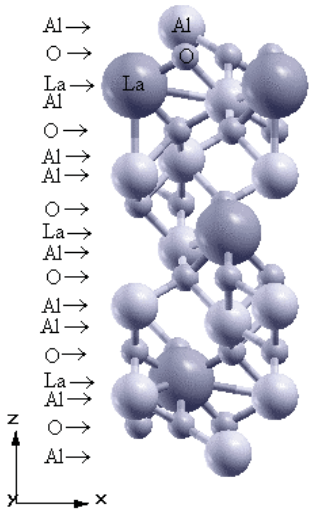

Fig. 2. The unit cell of α-$Al_{2-x}La_xO_3$ ($x = 0.5$) used in this study.

radial solutions of Schroedinger equation and their energy derivatives are used as basis functions, and an "interstitial" region between the muffin tins (MT) in which the basis set consists of plane waves. There is no pseudopotential approximation and core states are calculated self-consistently in the crystal potential. Also, core states are treated fully relativistically while valence and semi-core states are treated semi-relativistically (i.e. ignoring the spin-orbit coupling). The cut-off energy, which defines the separation of the core and valance states, was chosen as −6 Ryd.

3 Results and discussion

The pure α-alumina was first studied, and the calculations were performed with 400 k-points and $Rk_{\max} = 7$ for the convergence parameter, for which the calculations stabilized and convergence in terms of the energy was achieved. This gives well-converged basis sets consisting of approximately 2470 plane waves. Under these conditions the values of the other parameters were $G_{\max} = 14$, $R_{\mathrm{MT}}\,(\mathrm{Al}) = 1.7$ a.u, $R_{\mathrm{MT}}\,(\mathrm{La}) = 1.8$ a.u, $R_{\mathrm{MT}}\,(\mathrm{O}) = 1.7$ a.u. The iteration halted when the total charge was less than 0.0001 between steps.

3.1 Pure α-Al_2O_3

3.1.1 Dielectric function

We calculated both electronic and optical properties of pure α-Al_2O_3 and La aluminates, but here we only present the optical properties. The detailed description for the electronic properties is given elsewhere [15].

The complex dielectric tensor was calculated, in this program, from the following equations [13]:

$$\mathrm{Im}\varepsilon_{\alpha\beta}(\omega) = \frac{4\pi e^2}{m^2\omega^2} \times \sum_{c,v} \int dk \,\langle c_{\mathbf{k}}|p^{\alpha}|v_{\mathbf{k}}\rangle \left\langle v_{\mathbf{k}}|p^{\beta}|c_{\mathbf{k}}\right\rangle \delta(\varepsilon_{c_{\mathbf{k}}} - \varepsilon_{v_{\mathbf{k}}} - \omega) \quad (1)$$

$$\mathrm{Re}\varepsilon_{\alpha\beta}(\omega) = \delta_{\alpha\beta} + \frac{2}{\pi} P \int_0^{\infty} \frac{\omega' \mathrm{Im}\varepsilon_{\alpha\beta}(\omega')}{\omega'^2 - \omega^2} d\omega' \quad (2)$$

and the optical conductivity from equation (3):

$$\mathrm{Re}\sigma_{\alpha\beta}(\omega) = \frac{\omega}{4\pi}\mathrm{Im}\varepsilon_{\alpha\beta}(\omega). \quad (3)$$

In equation (1), c_k and v_k are the crystal wavefunctions corresponding to the conduction and the valance bands with crystal wave vector $\mathbf{k}$ (Fig. 4).

The real and the imaginary parts of the dielectric functions are shown in Figure 3 for pure α-Al_2O_3. The small circles are calculated in this work, the solid line is taken from Ahuja et al. [1] based on the full-potential linear muffin-tin-orbital (FP-LMTO) method, and the dashed line is taken from experimental values [1]. The calculated results of $\varepsilon_1(\omega)$ (in principle) are similar with reference [1]. However, as indicated by Ahuja, the steep slope near the absorption edge and the sharp peak in the experimental spectrum are absent. This is probably because that the calculation only involves the interband transition from valance to conduction band states. The calculated $\varepsilon_2(\omega)$ shows three main peaks at about 12, 13 and 15.6 eV, and is rather smooth at higher energy. There is a constant difference between experimental data and the calculated results. This deviation, however, from a critical review of the experimental and theoretical investigations becomes evident. The measured fundamental energy gap of α-Al_2O_3

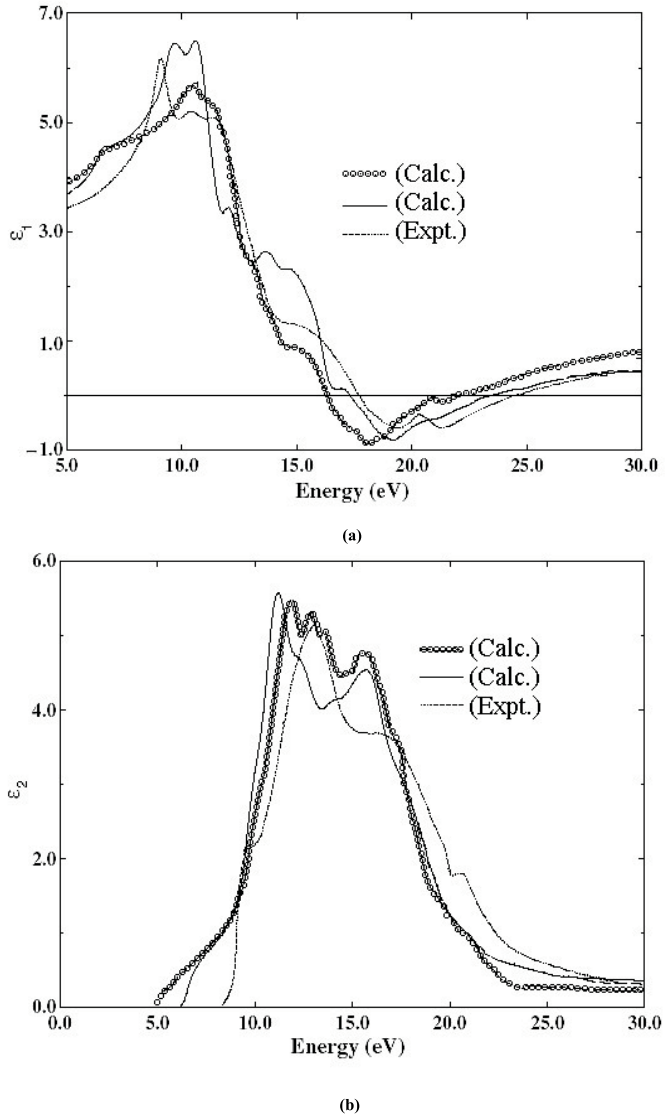

Fig. 3. (a) Real, (b) Imaginary part of dielectric function for pure α-Al_2O_3. Small circles this work, solid and dashed line [1].

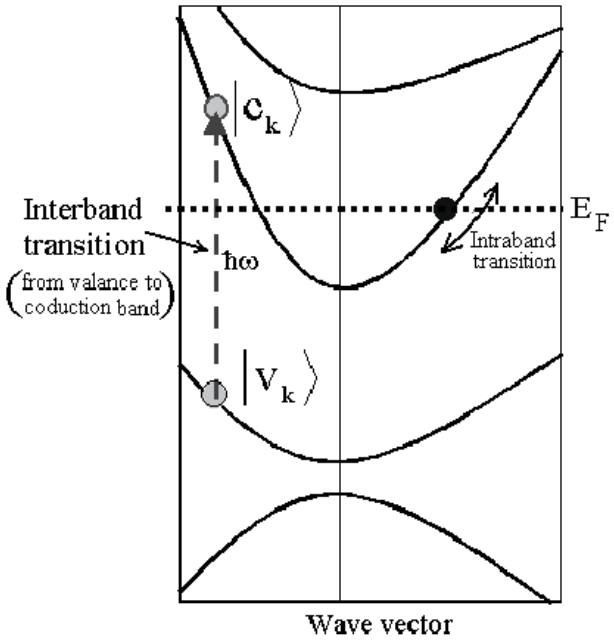

Fig. 4. Valence interbands transitions.

Table 1. α-Al_2O_3 static refractive index calculated by various methods.

Methods	Static refractive index (n_0)
Experimental	
KK analysis of EELS data [5]	∼1.78
Theory	
Optical Properties [3]	∼1.77
FP-LMTO [1]	∼1.79
OLCAO [2]	∼1.96
FP-LAPW (GGA96) (this work)	∼1.64

is about ∼9 eV, while in this method (without scissors operation) is found to be 6.4 eV, as reported in our previous work [15]. If we use the scissors operation and shift the calculated curve rigidly by about 2.5 eV, then the spectrum is in a better agreement with the experimental data.

The static refractive index value for pure α-Al_2O_3 calculated in this work, and the values obtained by other methods are summarized in Table 1.

3.1.2 Electron Energy Loss Spectroscopy

EELS is a valuable tool for investigating various aspects of materials [14]. It has the advantage of covering the complete energy range including non-scattered and elastically scattered electrons (Zero Loss), electrons, which excite the atoms electrons of the outer shell (Valence Loss) or valence interband transitions (Fig. 4). Also the fast electrons excite the inner shell electrons (Core Loss) or induce core level excitation of Near Edge Structure (ELNES) and XANES.

In the case of interband transitions, which consists mostly of plasmon excitations, the scattering probability for volume losses is directly connected to the energy loss function. One can then calculate the EEL spectrum from the following relations [13]:

$$\varepsilon_{\alpha\beta}(\omega) = \varepsilon_1 + i\varepsilon_2$$
$$\text{and} \quad \text{EEL Spectrum} = \text{Im}[-1/\varepsilon_{\alpha\beta}(\omega)] = \frac{\varepsilon_2}{\varepsilon_1^2 + \varepsilon_2^2}. \qquad (4)$$

In Figure 5 the energy loss function is plotted for pure α-Al_2O_3. The energy of the main maximum of $\text{Im}[-\varepsilon^{-1}(E)]$ is assigned to the energy of volume plasmon $\hbar\omega_p$. The value of $\hbar\omega_p$ obtained in this work and by others is given in Table 2.

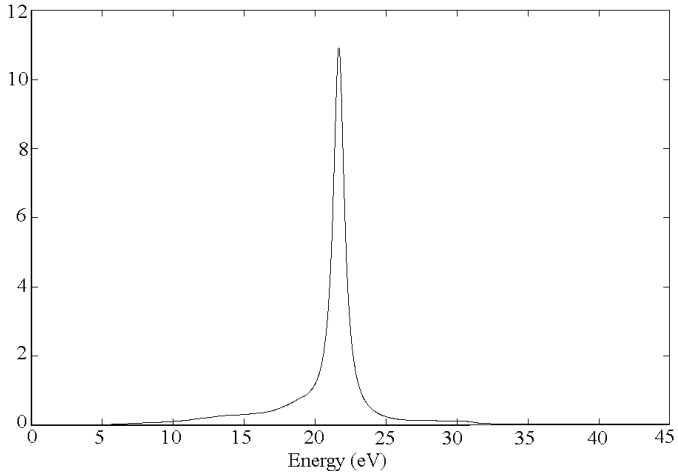

Fig. 5. Electron energy loss spectrum $\mathrm{Im}[-\varepsilon^{-1}(E)]$ for pure α-Al_2O_3.

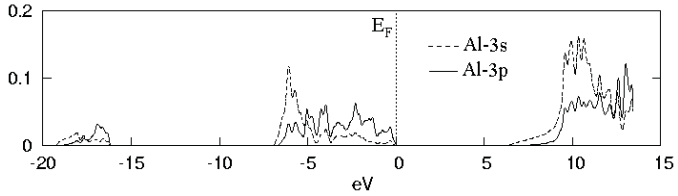

Fig. 6. The partial DOS of Al-3s and Al-3p.

Table 2. α-Al_2O_3 plasmon energy $\hbar\omega_p$ of the energy loss function calculated by various methods.

Methods	Plasmon energy $\hbar\omega_p$ (eV)
Experimental	
VUV Spectroscopy [5,12]	∼26.0
Theory	
OLCAO [2]	∼25.0
FP-LAPW (GGA96) (this work)	∼21.4
Free electron	∼27.9

For free electrons the plasmon energy is calculated according to the following model:

$$\hbar\omega_p^e = \hbar\sqrt{\frac{ne^2}{\varepsilon_0 m}}. \tag{5}$$

If we use this model, then what should be the number of valance electrons per Al_2O_3 molecule, N, used to calculate the density of valance electrons, n, and thus the plasmon energy in equation (5)? The partial DOS from the Al and O atoms are shown in Figures 6 and 7. From the PDOS of the O-atoms it can be seen that the O-2s state has a narrow band separated from the upper valance band by nearly −11 eV, therefore the participation of the O-2s state in the volume plasmon excitation is rather weak. If we take only the contribution of $3p^1$ and $3s^2$ electrons of Al, and $2p^4$ of O (ignoring the contribution of $2s^2$ electron of O atom)

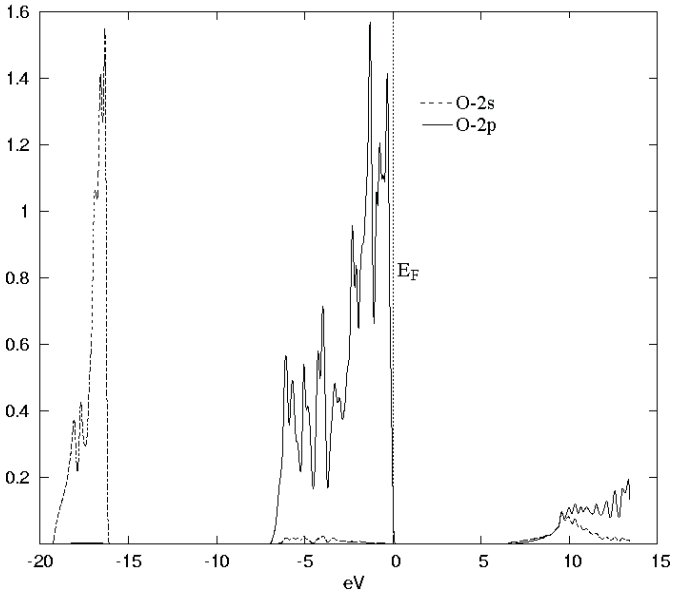

Fig. 7. The partial DOS of O-2s and O-2p.

then we have $N = 18$ and the free electron plasmon energy will be 24 eV. Otherwise, with $3p^1$, $3s^2$ electrons of Al and $2p^4$, $2s^2$ electrons of O atom (i.e. $N = 24$), the free electron plasmon would be 27.9 eV, as indicated in Table 2. We will also see from sum rule data that $N = 18$ is a reasonable value for the valance electrons per Al_2O_3 molecule.

Referring to Table 2, it can be seen that the calculated plasmon energy in this work is smaller than the values measured experimentally. This difference may be mainly due to the calculated band gap value 6.4 eV, which is about 2.5 eV less than the experimental value, as already reported [15].

3.1.3 Oscillator strength sum rule

Another way to consider the number of electrons involved in the valance interband transition is to evaluate the sum rule. The effective number of valance electron per unit cell contributing to a transition up to energy E can be calculated using the sum rule [13]:

$$n_{eff}(E) = \frac{2m}{Ne^2h^2}\int_0^E E\mathrm{Im}[\varepsilon(E)]dE \tag{6}$$

where m and e are the electron mass and charge respectively and N is the electron density. The oscillator strength sum rule for α-Al_2O_3 is shown in Figure 8. The effective electron number up to 6.63 eV is zero (below band gap) then rises rapidly at low energy and saturates at about 20 eV, with a value of 16 for the effective electron number. However, in this transition, the contribution of O-2p bands to $n_{eff}(E)$ is the largest, followed by Al = O hybridized bands, and finally the O-2s bands contribution which is least.

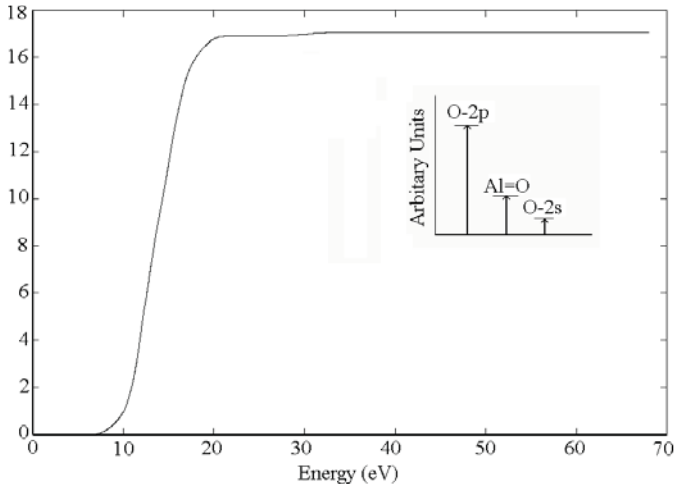

Fig. 8. Calculated oscillator strength sum rule for α-Al_2O_3.

The relatively small $n_{eff}(E)$ confirms, to some extent, the assumption that we may ignore the contribution of the O-2s state. This is due to the stronger localization of deep lying O-2s state, which inhibits transfer at low energies to high-energy interband transitions (Fig. 7) However, this result is very close to experimental value measured from VUV spectroscopy and EELS data in which 16.8 electrons with transitions up to 42 eV [5] are reported.

3.2 La aluminates

3.2.1 Dielectric function

Figure 9 shows the real and imaginary parts of the dielectric functions for La aluminates.

The general behavior of $\varepsilon_1(\omega)$ for La aluminates curve is similar to that for pure α-Al_2O_3. In this case, there are two extra peaks at 11 eV and 18 eV associated with La-5 and La-6s orbital inter-band transitions, respectively. The main peak of $\varepsilon_2(\omega)$ for La aluminates is in good agreement with the experimental value for pure α-Al_2O_3, except for these two extra peaks. This means that due to the extra state as a result of La doping, the band gap is decreased, and therefore, in order to apply the scissors operation, the rigid shift should be about 3 eV. The static dielectric constant for La aluminates has been increased to 1.73.

3.2.2 Electron Energy Loss Spectroscopy

In Figure 10 the energy loss function is plotted for La aluminates. The energy of the main maximum of $\mathrm{Im}[-\varepsilon^{-1}(E)]$, or the energy of volume plasmon $\hbar\omega_p$, is equal to that for pure α-Al_2O_3 (21.6 eV). However, there is another peak at lower energy, 17.8 eV, which is mainly due to the La valance state. The free electron plasmon energy calculated according to equation (5) for La aluminates with $5d^1$ and $6s^2$ states of La, is 26.7 eV, which is smaller than for pure α-Al_2O_3. This is associated with the smaller number of valance electrons for the of $Al_{1.5}La_{0.5}O_3$ molecule.

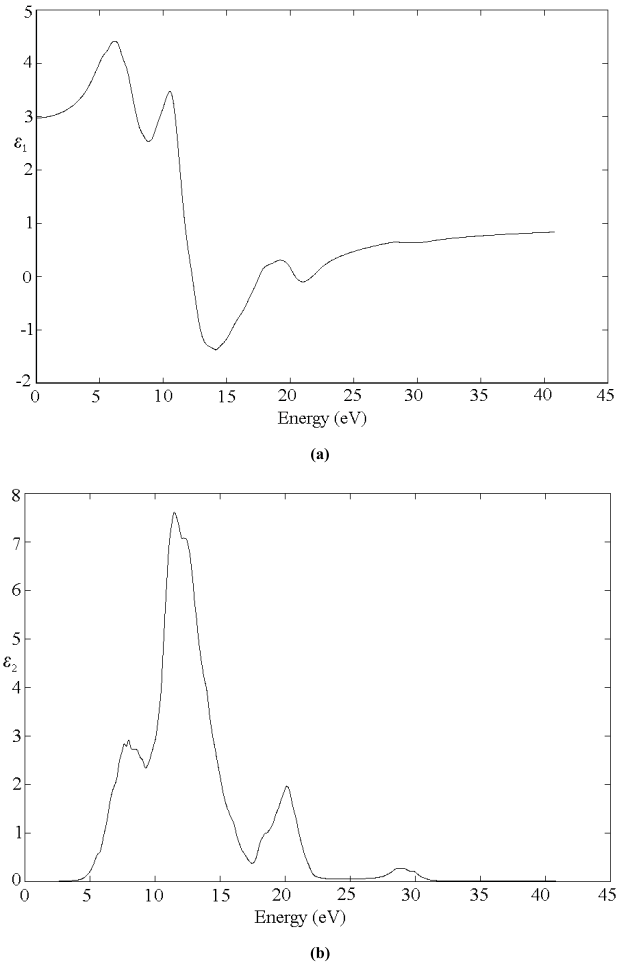

Fig. 9. (a) Real (b) Imaginary part of dielectric function for $Al_{1.5}La_{0.5}O_3$.

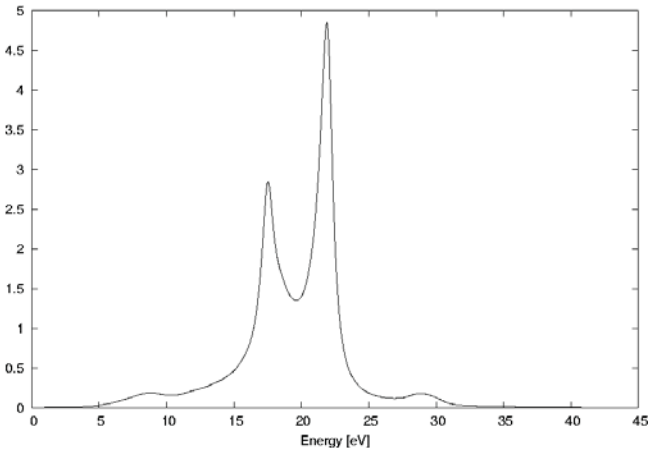

Fig. 10. Calculated EELS for La aluminates.

As we can see from the total DOS of the La atoms, Figure 11, the La-6s^2 state is localized though as deep lying as the O-2s state and the probability to transfer at low energy to high-energy interband transitions is less likely.

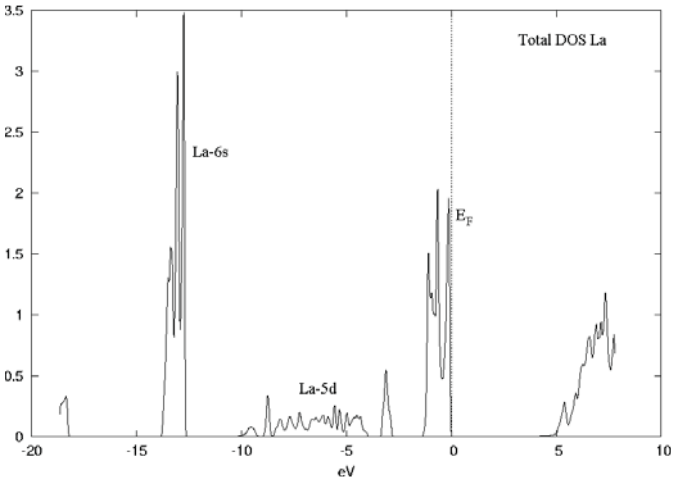

Fig. 11. Calculated total DOS for La atom.

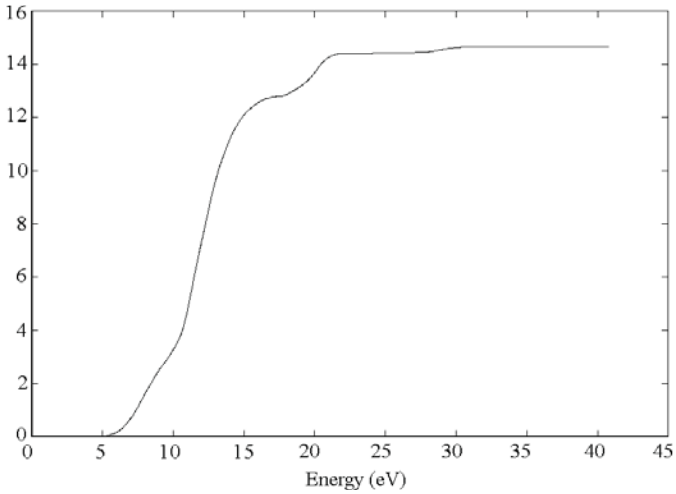

Fig. 12. Calculated oscillator strength sum rule for La aluminates.

3.2.3 Oscillator strength sum rule

Figure 12 shows the $n_{eff}(E)$ for La aluminates. There is also a small change in the results of the sum rule between 16 to 22 eV, mainly due to La-$5d^1$ and $6s^2$ state. The plasmon energy of free electrons calculated for La aluminates with $5d^1$ and $6s^2$ states for La is 26.7 eV. The relatively small $n_{eff}(E)$ again confirms, to some extent, the assumption that we may ignore the contribution of the O-2s state in La aluminates.

Substitution of La for Al in α-Al_2O_3 results in a reduction of the band gap and as a result, the number of effective electron, $n_{eff}(E)$, is zero (up to about 5 eV, below band gap). It rises rapidly at low energy to a value near 16 eV, and then there is another rise, and finally, saturation at a value near 22 eV with a value of 14.4 for the effective electron number. However, in this transition, the contribution of O-$2p^4$ bands to $n_{eff}(E)$ is most dominated then Al = O hybridized bands, followed by La-$5d^1$, while La-$6s^2$ is less, and finally, the contribution of O-$2s^2$ band is least.

4 Conclusions

We have calculated the optical properties of pure α-Al_2O_3 and La aluminates ($Al_{2-x}La_xO_3$, $x = 0.5$) using the full potential–linearized augmented plane wave (FP-LAPW) method with the generalized gradient approximation (GGA). The calculations show a static refractive index of 1.64 and an EEL spectrum of 21.6 eV. The effective electron number at low energy saturates near 20 eV with the value of 16 for the effective electron number. The substitution of La for Al increases the static refractive index to 1.73 for $Al_{1.5}La_{0.5}O_3$, and this is mainly due to the number of states originating from the La-d state in the conduction band. The effective electron number up to 5 eV is zero and rises rapidly at low energies to a value near 16 eV then rise again and saturates at about 22 eV with the value of 14.4 for the effective electron number.

The authors are grateful to Professor P. Blaha (at Vienna University of Technology Austria) for his technical assistance in the use of Wien2k package.

References

1. R. Ahuja, J.M. Osorio-Guillen, J.S. Almeida, B. Holm, W.Y. Ching, B. Johansson, J. Phys.: Condens. Matter **16**, 2891 (2004)
2. W.Y. Ching, Y.N. Xu, J. Am. Ceram. Soc. **77**, 404 (1994)
3. S.-D. Mo, W.Y. Ching, R.H. French, J. Phys. D **29**, 1761 (1996)
4. H. Müllejans, R.H. French, Interband, J. Phys. D **29**, 1751 (1996)
5. R.H. French, H. Mullejans, D.J. Jones, J. Am. Ceram. Soc. **81** (10), 2549 (1998)
6. M.E. Innocenzi, R.T. Swimm, M. Bass, R.H. French, A.B. Villaverde, M. R. Kokta, J. Appl. Phys. **67**, 7542 (1990)
7. R.H. French, D.J. Jones, S. Loughin, J. Am. Ceram. Soc. **77**, 412 (1994)
8. A. Kokalj, J. Mol. Graphics Modelling **17**, 176 (1999)
9. J.P. Perdew, J.A. Chevary, S.H. Vosko, K.A. Jackson, M.R. Pederson, D.J. Singh, C. Fiolhais, Phys. Rev. B **46**, 6671 (1992)
10. M. Peterson, F. Wanger, L. Hufnagel, M. Scheffler, P. Blaha, K. Schwarz, Computer Phys. Commun. **126**, 294 (2000)
11. P. Blaha, K. Schwarz, WIEN2k, Vienna University of Technology Austria (2002)
12. W. Tews, R. Grundler, Phys. Stat. Sol. (b) **109**, 255 (1982)
13. F. Wooten, *Optical properties of solids* (Academic Press, New York, 1972)
14. S. Loughin, R.H. French, L.K. Noyer, W.-Y. Ching, Y.-N. Xu, J. Phys. D: Appl. Phys. **29**, 1740 (1996)
15. S.M. Hosseini, H.A. Rahnamaye Aliabad, A. Kompany, *Influence of La on electronic structure of a-Al_2O_3 high k-gate from first principles*, Ceramics International, article in press (2004)